Iranian Hydraulic Association
Journal of Hydraulics

Research Article
https://doi.org

Modeling the Discharge Coefficient of Rectangular Labyrinth Weirs with FLOW-3FLOW-3D Simulation of Discharge Coefficient in Rectangular Labyrinth Weirs

Hossein Elahifar[1], Roozbeh Aghamajidi[2], Sajjad Amiri[3]

1- PhD, Dept. of Water Engineering, Islamic Azad University of Kerman Branch, Kerman, Iran, Email: elahifar@areeo.ac.ir, ORCID: 0000-0001-7154-7028.

2- Assistant Professor, Civil Engineering, Islamic Azad University, Sepidan Branch, Sepidan, Iran, Email: roozbeh1381@yahoo.com, ORCID: 0000-0003-1759-7870.

3- MSc, Water Engineering, Sarzamin Sabz Paydar Consulting Engineers Company, Ahvaz, Khouzestan, Iran, Email: sajjadamiri1986@gmail.com, ORCID: 0000-0003-4402-1439.

*** roozbehaghamajidi1396@gmail.com**

Abstract

Labyrinth weirs are specialized hydraulic structures widely employed in canals, rivers, and dam reservoirs to effectively regulate upstream water levels and manage flow discharge. Their folded, zigzag configuration significantly extends the effective crest length within a constrained channel width, thereby enhancing discharge capacity compared to conventional linear weirs. To investigate their hydraulic performance numerically, this study utilized FLOW-3D software, a powerful computational fluid dynamics (CFD) tool capable of simulating complex free-surface flows, turbulence, and weir interactions.

Dimensional analysis based on the Buckingham Pi theorem identified the discharge coefficient (Cd) as a key performance parameter dependent on several dimensionless hydraulic and geometric variables. These include the ratio of total upstream head to weir height (Ht/P), the left-to-right cycle width ratio (WL/WR), and the longitudinal weir length ratio (B/Wavg), defined as the sidewall length relative to the average cycle width. Physical experiments were conducted in a rectangular flume measuring 8 m long, 0.6 m wide, and 0.6 m high to gather benchmark data. The corresponding physical setup was then replicated in FLOW-3D for numerical modeling. Results demonstrated strong agreement between the experimental and numerical outcomes, validating the model's accuracy in capturing flow behavior over the weir.

Notably, in symmetrical labyrinth weirs, the discharge coefficient obtained from physical modeling was approximately 27% higher than that from numerical simulations, potentially due to differences in turbulence modeling, boundary effects, or minor discrepancies in nappe aeration and surface tension representation. Furthermore, numerical results indicated that asymmetric labyrinth weirs (with unequal cycle widths) exhibited a discharge coefficient about 16% higher than their symmetric counterparts. This improvement

in asymmetric designs likely arises from altered flow patterns that reduce adverse interference between adjacent channels, minimize local submergence, and promote more efficient nappe discharge under certain conditions. These findings underscore the potential of asymmetry to optimize labyrinth weir efficiency in space-limited or site-specific applications, while highlighting the complementary value of combining physical experiments with CFD simulations for reliable hydraulic design.

Keywords: Labyrinth weirs, hydraulic head, discharge coefficient, asymmetric and symmetric rectangular labyrinth weir.

1. Introduction

One of the problems faced by irrigation and drainage networks is the change in the discharge of the intake structure in terms of severe fluctuations in water level in the main flow direction. Labyrinth weirs are among the hydraulic structures to regulate the water level and flowcontrol in canals, rivers, and dam reservoirs. Regarding the relationship between the overflow and the hydraulic head in the weirs, increasing the crest length of the weir is one way to reduce the fluctuations caused by the changes in the discharge. Labyrinth weirs are often used with rectangular, trapezoidal, and triangular planes. The discharge coefficient of labyrinth weirs depends on several parameters, including the hydraulic and geometric characteristics of the weirs. The hydraulic performance of free overflows for a constant head is directly related to the weir length and the discharge coefficient (C_d) of this type of weir is determined by Equation (1).

$$Q = \frac{2}{3} \times \sqrt{2g} \times Cd \times L \times H_t^{1.5} \quad (1)$$

In equation 1, (Q) discharge, (C_d) discharge coefficient, (g) gravity acceleration, (H_t) total hydraulic head and (L) is crest length. Figure 1 shows geometric and hydraulic parameters of a rectangular labyrinth weir in the 3D view, plan and profile view of the weir.

Savage et al. (2016) investigated Physical and numerical modeling of large headwater ratios for a 15° labyrinth weir. The physical and numerical data provide practical design guidance for high headwater ratios and indicate that the empirical discharge coefficient design curves developed by Crookston may be acceptable for headwater ratios up to 2.0 or more. This was done by examining the effects of increased upstream heads on a 15° sidewall angle labyrinth weir. The physical and numerical models were found to correspond quite well. The results of numerical model indicate that the selected turbulence models had very little effect on discharge. The comparison of physical and numerical model results advocate that a numerical model can provide a good approximation of the expected discharge, especially at the higher heads. The ability to numerically model a design or analyze an existing weir allows site-specific characteristics (e.g., differing approach velocities or weir geometries) to be evaluated without the construction of a scaled physical model. However, the authors encourage that a numerical model is validated. Furthermore, the benefits of composite modeling should not be overlooked.

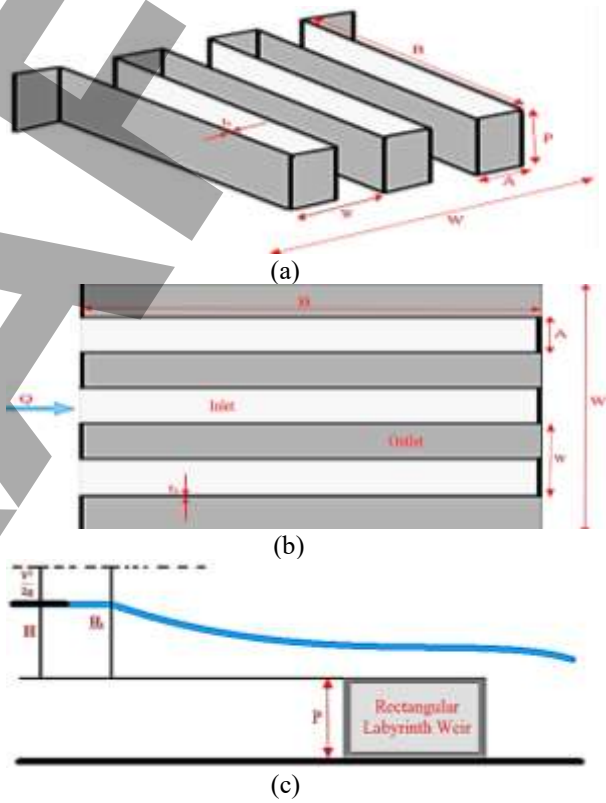

Fig. 1 a) 3D view, b) plan view, and c) labyrinth weir profile.

Zamiri et al. (2018), studied the effect of shape changes in the plan of

This study utilized the FLOW-3D numerical simulation software to explore ways to enhance the hydraulic efficiency of labyrinth weirs, which are zigzag-shaped spillway structures designed to increase water discharge capacity within a limited channel width by extending the effective crest length. The researchers first validated their model by simulating a labyrinth weir with a very sharp sidewall angle of 6° (creating narrow, elongated channels) and confirmed its accuracy against experimental data from prior studies. They then

examined variations in performance by testing weirs with wider sidewall angles of 45° and 85°, as well as different apex (corner) shapes: triangular, half-circular, and the conventional linear (straight-edged) form. The discharge coefficient (Cd), a key measure of how efficiently the weir passes water for a given upstream head, served as the primary performance indicator.

The results revealed that labyrinth weirs with larger sidewall angles (45° and 85°) achieved significantly higher discharge coefficients than the sharp 6° configuration, indicating better flow efficiency due to reduced interference, less contraction, and lower energy losses in the wider-angled designs. Additionally, modifying the apex shape proved highly beneficial: the triangular apex improved the discharge coefficient by approximately 50.29%, while the half-circular (semicircular) apex provided a modest gain of about 4.15%, both relative to the standard linear apex. These enhancements stem from smoother flow guidance at the corners, minimized local turbulence, and reduced nappe interference or submergence effects. Overall, the findings highlight practical geometric optimizations—favoring wider sidewall angles and especially triangular apexes—that can substantially boost labyrinth weir performance for applications like flood control and dam spillways, with FLOW-3D offering an effective, cost-efficient tool for such design explorations.

Gharibvand et al. (2018), studied on Numerical Analysis of Flow Hydraulic in Trapezoidal Labyrinths and Piano Key Weirs. The results showed good agreement between the data from the numerical and experimental models. The piano key weirs had a higher coefficient of discharge compared with labyrinth weirs. The coefficient of discharge was observed to increase by 26 percent as the height of PKW was increased by 50 percent (from 5 to 7. 5 cm). This increase was 24 percent for labyrinth weirs.

Recent advancements in labyrinth weir research have heavily relied on numerical modeling using computational fluid dynamics (CFD) tools like FLOW-3D to complement and sometimes replace costly physical experiments. These studies focus on validating simulation accuracy, understanding flow patterns under free and submerged conditions, and exploring geometric optimizations for improved discharge performance. For example, **Carrillo et al. (2020)** conducted detailed CFD simulations of labyrinth weirs with large sidewall angles, testing free-flow and submerged regimes across different turbulence models (including RNG κ-ε). Their findings showed excellent agreement with experimental data, with relative differences in discharge coefficient (**Cd**) below **1%** for free flows and up to **3.6%** for submerged conditions. Notably, the normalized upstream free surface profile remained nearly constant regardless of the head-to-weir height ratio (**Ht/P**) in free-flow scenarios. In submerged flows, dimensionless submerged heads from the simulations aligned closely with prior experimental results (e.g., Lopes, 2011) and regression equations (e.g., Tullis et al., 2007). Such high-fidelity validations demonstrate that modern CFD can reliably predict complex weir hydraulics, including nappe behavior, turbulence, and submergence effects, reducing reliance on large-scale physical models.

Geometric modifications play a critical role in enhancing labyrinth weir efficiency, particularly at varying hydraulic heads. Ghaderi et al. (2020) validated a numerical model with a maximum relative error of 4.8% against experiments, confirming CFD's suitability for flow prediction over modified labyrinth weirs. Their simulations revealed that at low Ht/P ratios (especially < 0.2), changes like increased cycle length-to-width ratios (Lc/wc) boost the discharge coefficient and flow magnification (Q/Qn, where Qn is conventional weir discharge) by improving flow passage and reducing interference. However, as Ht/P increases, performance declines sharply due to vortex generation, upstream flow rejection, and local submergence in entrance cycles, limiting overall capacity. Tullis et al. (2020)

further examined geometric influences, finding that hydraulic efficiency decreases with more cycles in a fixed-width channel because of increased interference and energy losses. Upstream apex shapes proved more impactful on efficiency than downstream ones, while weir height effects were nuanced: very short heights impair performance through excessive contraction or aeration issues, but taller weirs offer gains only up to an optimal point beyond which diminishing returns or negative effects (e.g., increased friction or submergence) occur.

Supporting literature reinforces these trends in labyrinth (or congruent) weir design. Studies using FLOW-3D on trapezoidal arced labyrinth weirs with varying middle cycles have shown good agreement between numerical and experimental discharge coefficients, though numerical values are often slightly lower, with discrepancies growing at larger arc radii due to modeling challenges in curvature and flow separation (Feili et al., 2024). Experimental investigations into geometric parameters—such as sidewall angles (**α**), weir height (**P**), apex/nose shapes, crest profiles, and inlet slopes—indicate that smaller sidewall angles (e.g., 12°) yield lower **Cd** compared to larger ones (e.g., 20° or 35°), as wider angles allow flow to approach more perpendicularly, mimicking linear weirs and reducing interference (Kougdaragh, 2025). Collectively, these works highlight practical strategies for engineers: prioritize fewer cycles, optimized apex/crest geometries, and low-head operation to maximize discharge capacity in space-constrained spillways for flood control, irrigation, or reservoir management.

Mahmoud et al. (2021), studied discharge capacity and the LS concrete volume was considered as two objective functions, and the Ute dam LS was investigated as the case study. They expressed despite higher confidence of MLP-LM in the testing stage, it reports unrealistic Q; on average, 350 m3/s and 280 m3/s higher than RBFNN and MLP-FA, respectively. Applying MOP to the Ute labyrinth spillway leads to a set of optimal designs that all are dominating Ute LS original design.

The present study aimed to numerically investigate the discharge coefficient of symmetrical and asymmetric labyrinth weirs by using FLOW-3D software, the results of which were validated with the results of physical modeling.

2 Materials and Methods

2.1. Physical Modeling

Experimental data were obtained using physical modeling and the results are represented in the form figure2. Physical modeling tests were performed on the flume with 8 m length, 0.6 m width, and 0.6 m height. The discharge was measured with a manometer located inside the downstream v-notch weir. The upstream and downstream hydraulic heads were measured with point gauges, with ± 0.05 mm resolution. Figure 2 shows the plan and profile of the experimental flume. In Figures 2a and 2b, Inlet Tank (1), Experimental Flume (2), Outlet Tank (3), Underground Tank (4), Manometer (5), Head Tank (6), PE Pipe (7), Experimental Flume (8), Valve (9), Point gauge (10) and Energy Dissipater (11).

The physical model of labyrinth weirs was made with 3-mm-thick Plexiglas (Figure 3). Table 1 shows the geometric and hydraulic characteristics of labyrinth weirs to better understand physical model dimensions.

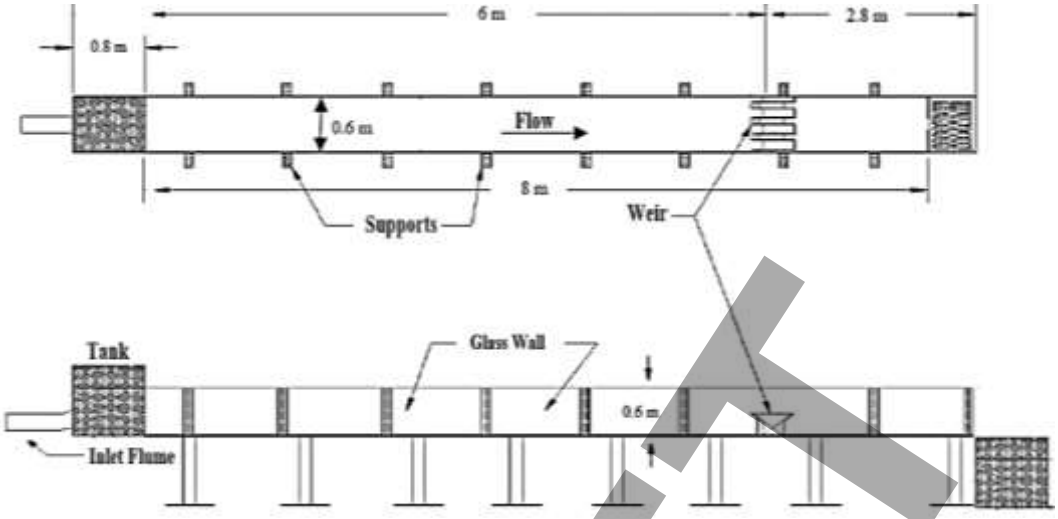

(a)

(b)

Figure 2. a) The plan and longitudinal profile of the experimental flume, b) Flume components and supporting installations.

Table 1. Geometric and hydraulic characteristics of labyrinth weirs.

Type of Labyrinth Weir	No.	B (cm)	w (cm)	B/W_{avg}	W_L (cm)	W_R (cm)	W_L/W_R	W_{avg} (cm)	t_s (mm)	N	P (cm)	Number Of Discharge	Number Of Tests
Symmetric rectangular	1	90	58	3.1	29	29	1	29	3	2	10	12	12
Asymmetric rectangular	2	80	58	2.76	36.5	21.5	1.7	29	3	2	10	12	12

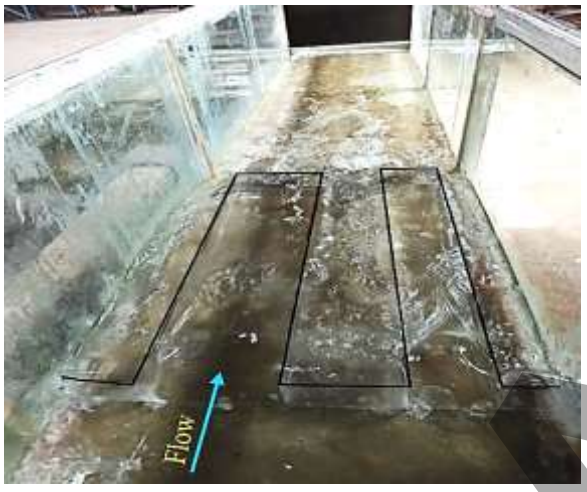

Fig. 3 Asymmetric rectangular labyrinth weir

Dimensional analysis is one of the basic steps for physical and numerical modeling. Dimensionally variable parameters were determined using dimensional analysis by Buckingham method. The effective parameters on the discharge coefficient of labyrinth weirs are shown in Equation (2).

$$C_d = f\ (Q\ ,\ B\ ,\ S\ ,\ W_L\ ,\ W_R\ ,\ w\ ,\ W_{avg}\ ,\ t_s\ ,\ P\ ,\ N\ ,\ H_t\ ,\ g\ ,\ \mu\ ,\ \rho\ ,\ \sigma) \quad (2)$$

Where the discharge coefficient (C_d) is a function of discharge (Q), length of the lateral crest (B), bottom slope (S), the left cycle width (W_L), right cycle width (W_R), average width of left and right cycles (W_{avg}), the total weir width (W), weir wall thickness (t_s), weir height (P), number of cycles (N), total hydraulic head (H_t), gravitational acceleration (g), dynamic viscosity (μ), fluid density (ρ), and the fluid surface tension (σ). In the dimensional analysis, (ρ), (P) and (Q) were considered as repeating variables. The dimensionless parameters are, therefore, expressed in Equation (3).

$$C_d = f\ (B/P\ ,\ t_s/P\ ,\ W_L/P,\ W_R/P\ ,\ W_{avg}/P\ ,\ N\ ,\ H_t/P\ ,\ S\ ,\ gP^5/Q^2\ ,\ \mu P/\rho Q\ ,\ w/P\ ,\ \sigma/\rho P) \quad (3)$$

The left cycle width ratio (W_L/P) and right cycle width ratio (W_R/P) were combined to produce a dimensionless and varying parameter, i.e. width ratio of the left and right cycles (W_L/W_R). Further, combining the lateral crest length (B/P) with the average of left and right cycle width ratio (W_{avg}/P) produced the dimensionless variable B/W_{avg}. In this regard, most references, including the American Society of Civil Engineers (ASCE, 2000), recommend a minimum 2.5 cm hydraulic head for this purpose. After removing the dimensionless constants, Equation 4 was presented as the final equation to calculate the discharge coefficient:

$$C_d = f\ (W_L/W_R\ ,\ H_t/P\ ,\ B/W_{avg}) \quad (4)$$

Where (C_d) defines the coefficient of discharge, (H_t/P) is the total hydraulic head ratio (total hydraulic head to the weir height), (W_L/W_R) is the width ratio of the left and right cycles, and (B/w_{avg}) is the weir length ratio (ratio of the lateral crest length to the average length of the weir cycle).

2.2 Numerical Modeling

The rapid evolution of computational capabilities has propelled Computational Fluid Dynamics (CFD) into a cornerstone of modern fluid mechanics, transforming it from an emerging specialty into an indispensable engineering tool. By numerically solving the full Navarro-Stokes

equations—which describe the conservation of mass, momentum, and energy in fluid flows—CFD employs sophisticated discretization schemes (finite volume, finite difference, or finite element) to simulate highly complex phenomena with remarkable detail. For hydraulic structures such as weirs and spillways, particularly labyrinth configurations, CFD now stands as a superior, cost-efficient alternative to traditional physical modeling. Advances in processor speed, parallel computing, and optimized algorithms enable engineers to evaluate site-specific weir designs rapidly and economically, often at a fraction of the expense associated with constructing, instrumenting, and testing scaled physical models in large flumes. Critically, CFD provides comprehensive, high-resolution data across the entire flow domain—including instantaneous velocities, pressure distributions, shear stresses, turbulence quantities, and hydrodynamic forces—metrics that are extremely challenging, intrusive, or prohibitively expensive to obtain experimentally due to probe interference, limited measurement points, or setup constraints. While early concerns about CFD's predictive accuracy persisted, extensive validations in recent literature (e.g., for labyrinth weirs using FLOW-3D) have demonstrated errors typically below 5–10% for discharge coefficients and flow patterns, affirming its reliability and growing acceptance as a design and optimization tool.

The inherent complexities of weir overflow—particularly the detachment of the nappe, formation of a free-falling jet, and the dynamic air-water interfaces on both sides—pose severe challenges for accurate numerical representation, demanding robust free-surface tracking to capture aeration, contraction, re-entrainment, and potential splashing or wave breaking. To overcome these difficulties, the commercial CFD package FLOW-3D (Flow Science) was selected for its proven excellence in multiphase free-surface simulations. At its core lies the Volume of Fluid (VOF) method, pioneered by Hirt and Nichols (1981), which efficiently tracks the interface by assigning a scalar volume fraction (0 to 1) to each cell, reconstructing the surface as a piecewise-linear plane oriented according to local gradients and neighboring fractions. This approach minimizes numerical diffusion while preserving sharp interfaces even under violent deformations. Complementing VOF, the Fractional Area/Volume Obstacle Representation (FAVOR) technique (Hirt & Sicilian, 1985) seamlessly incorporates intricate solid geometries—such as the folded walls and apexes of a labyrinth weir—into a structured Cartesian grid by computing fractional porosity and area coefficients in intersected cells, eliminating the need for computationally expensive body-fitted meshes.

The simulations solve the Reynolds-Averaged Navier-Stokes (RANS) equations within a finite-volume framework, incorporating the Renormalization Group (RNG) k-ε turbulence model (Yakhot & Orszag, 1986) for superior handling of separated flows, strong streamline curvature, and transitional turbulence regimes prevalent around labyrinth weirs. The computational domain was constructed as a hexagonal prism, discretized with a high-quality structured rectangular hexahedral mesh featuring three nested blocks to achieve adaptive resolution: coarser cells in uniform upstream regions and progressively finer grids near the weir to resolve rapid accelerations, boundary layers, free-surface curvature, and vortex structures with precision. Upstream boundary placement at approximately 50 cm from the crest ensured fully developed approach flow, while localized refinement minimized discretization errors in critical zones without excessive computational overhead. This setup closely mirrored the experimental configurations and methodologies of **Elahifar et al. (2022)** for symmetric/asymmetric rectangular

labyrinth weirs, enabling direct performance comparison and validation. Recent studies (2020–2025) using similar FLOW-3D setups for labyrinth and related weirs consistently report excellent agreement (relative errors often <5% for discharge, <10% for flow fields), underscoring the method's maturity.

For scenarios involving non-standard approach conditions—such as skewed inflows, reservoir projections, curved entrances, or complex bathymetry—empirical design equations like those from **Elahifar et al. (2022)** become unreliable due to unaccounted three-dimensional effects and interference. Physical modeling in these cases demands oversized headboxes, elaborate boundary treatments, and extensive instrumentation, driving costs and timelines prohibitively high. In contrast, CFD excels as a versatile, scalable alternative: it accommodates arbitrary geometries and boundary conditions at minimal additional expense, delivers full-field insights for diagnostic analysis (e.g., identifying stagnation zones or energy dissipation patterns), and supports parametric optimization to maximize discharge efficiency or mitigate adverse hydraulics. Table 2 details the mesh characteristics across blocks, while Figure 4 visualizes the nested hexahedral grid layout, illustrating how strategic refinement balances accuracy and efficiency in capturing the intricate, three-dimensional flow over the labyrinth weir.

Table 2. Grid Information for mesh block.

Block	Subject	Block	Total Number Of Real Cells	Minimum Cell Size	Maximum Cell Size	Maximum Adjacent Cell Size Ratio
1	X	1	85	0.00299978	0.0151067	2.33312
1	Y	1	57	0.00299999	0.01825	1.83907
1	Z	1	23	0.0105	0.0117143	1.0089
2	X	2	143	0.0174475	0.0174479	1.00003
2	Y	2	34	0.017647	0.0176471	1
2	Z	2	14	0.0175	0.0186111	1.00794
3	X	3	33	0.0179696	0.0179701	1.00003
3	Y	3	34	0.017647	0.0176471	1
3	Z	3	14	0.0178571	0.0178571	1

3 Results and discussion

Numerical modeling was performed using FLOW-3D software and the results were compared with experimental data of Elahifar et al. (2022).

3.1 Data validation

Figure 5 presents a detailed comparison of the discharge coefficient (Cd) for symmetric labyrinth weirs, derived from both physical (experimental) modeling and numerical (CFD) simulations. The plotted results demonstrate strong overall agreement between the two approaches across the tested range of hydraulic conditions, confirming the reliability of the numerical model in capturing the essential hydraulic behavior of the structure. In both experimental and numerical datasets, Cd exhibits a clear decreasing trend as the upstream hydraulic head increases. This reduction reflects the typical performance degradation of labyrinth weirs at higher heads, where increased interference between adjacent channels, nappe contraction, local submergence effects, vortex formation, and flow rejection upstream progressively limit the effective crest utilization and discharge efficiency.

A particularly noticeable pattern emerges when the hydraulic head ratio (Ht/P, where Ht is the total upstream head and P is the weir height) exceeds approximately 0.2. Beyond this threshold, the hydraulic efficiency of the symmetric labyrinth weir stabilizes into a consistent yet steadily declining trend. At lower Ht/P values (typically Ht/P < 0.2–0.3), the weir operates in a more efficient regime with minimal adverse interactions, allowing Cd to reach

relatively high peak values (often approaching or exceeding 1.0–1.2 depending on geometry). As Ht/P rises further, the channels experience greater submergence and energy losses, causing Cd to drop more pronouncedly—behavior well-documented in labyrinth weir literature and attributed to intensified three-dimensional flow complexities, such as sidewall effects and nappe interference.

Despite the good qualitative and quantitative alignment between physical and numerical results, a systematic discrepancy is evident: the discharge coefficient obtained from physical (laboratory) modeling is approximately 27% higher than that predicted by the numerical simulations across the range of tested conditions. This consistent overprediction in experiments relative to CFD could stem from several factors commonly observed in such comparisons. Physical models may benefit from more realistic nappe aeration, surface tension effects (especially at laboratory scales), or subtle boundary layer behaviors that are challenging to fully replicate in turbulence models (e.g., RNG k-ε in FLOW-3D). Numerical simulations, while excellent for capturing bulk flow patterns and free-surface dynamics via VOF, sometimes slightly underpredict Cd due to idealized boundary conditions, minor numerical diffusion, or incomplete representation of micro-scale phenomena like air entrainment or crest sharpness. Similar differences (though often smaller, e.g., 3–10%) appear in other labyrinth weir studies, but the 27% gap here highlights the value of combining both methods: experiments provide a benchmark "truth" under controlled conditions, while CFD offers scalable, detailed insights into flow fields, pressures, and optimization potential without the high costs of large-scale physical testing.

Overall, these findings reinforce the complementary strengths of physical and numerical approaches for labyrinth weir design. The strong correlation validates the CFD setup (including mesh refinement, turbulence modeling, and boundary treatments) as a trustworthy tool for preliminary analysis and parametric studies, particularly when validated against experiments like those referenced (e.g., Elahifar et al., 2022, for symmetric/asymmetric cases). The observed 27% offset suggests caution in applying numerical Cd values directly for final design without adjustment factors or hybrid calibration, especially in critical applications where precise discharge prediction is essential for flood safety or reservoir management. Future work could explore refined turbulence closures, scale effects, or enhanced aeration modeling to narrow this gap and further boost confidence in purely numerical predictions.

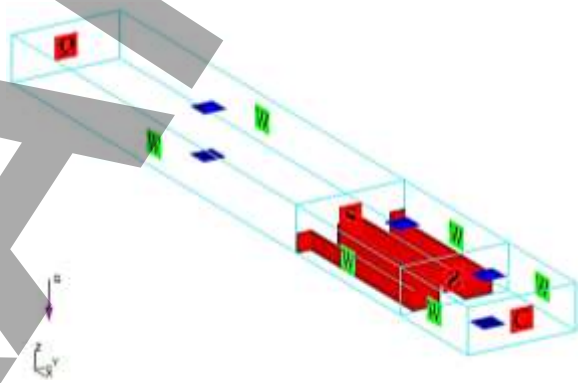

(a)

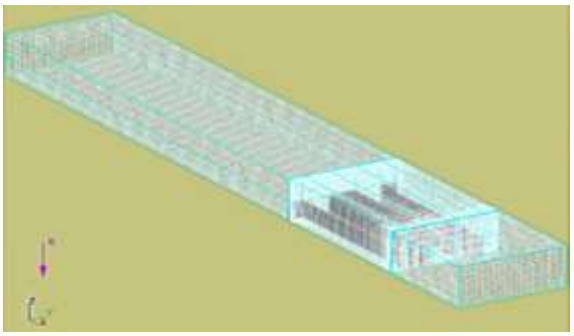

(b)

Fig. 4 a) Sketch Mesh Setup, b) Boundary Conditions for Labyrinth Weir.

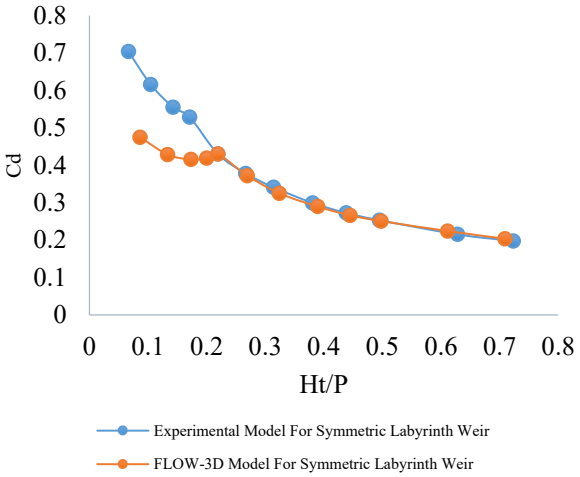

Fig. 5 Comparison of discharge coefficient for FLOW-3D model of symmetric labyrinth weir with results of Elahifar et al. (2022).

Figure 6 shows a comparison of the discharge coefficient values from physical and numerical modeling for an asymmetric labyrinth weir. The findings reveal by increasing the hydraulic head, the discharge coefficient decreases. The labyrinth weir passes through the stages of clinging and complete aeration in numerical and experimental simulation (The hydraulic head ratio is 0.06 to 0.16). At the same time, the results of numerical are in good agreement with experimental results.
The discharge coefficients for symmetric and asymmetric labyrinth weir are presented in Figure 7. As shown in Figure 7, the discharge coefficient is reduced by increasing hydraulic head ratio. The discharge coefficient of asymmetric labyrinth weir is roughly 12% greater than the symmetrical variety at a given hydraulic head ratio. In symmetric and asymmetric labyrinth weirs, discharge coefficient variations vary from 0.7 to 0.19. The results of numerical modeling for the discharge coefficients of symmetric and asymmetric labyrinth weir are presented in Figure 8. Figure 8 shows the discharge coefficient reduces by increasing hydraulic head. From the hydraulic head ratio (0.06 to 0.2), the weirs are in the stages of clinging and full aeration, and gradually from the value of 0.2 <, the weirs go through the stages of partial aeration and drown, respectively.

Figure 8 shows that the hydraulic efficiency of labyrinth weirs is very high at low hydraulic head ratios. Because asymmetric and symmetric labyrinth weirs have almost identical hydraulic processes, the asymmetric labyrinth weir has a 16 percent greater discharge coefficient than the symmetric kind at a given hydraulic head ratio.

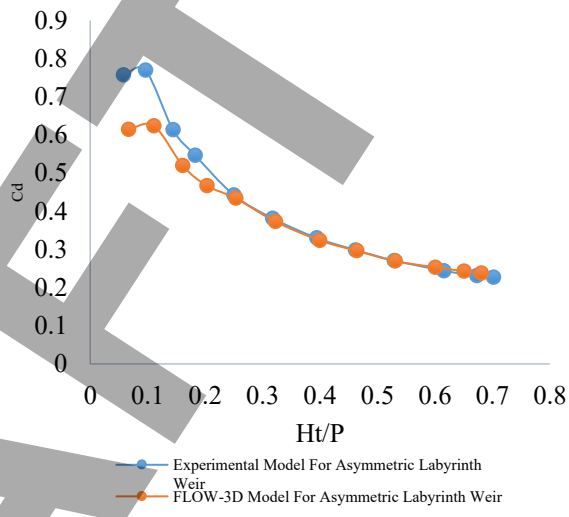

Fig. 6 Comparison of discharge coefficient for FLOW-3D model of asymmetric labyrinth weir with results of Elahifar et al. (2022).

The graph illustrates the variation of the discharge coefficient (Cd) as a function of the dimensionless hydraulic head ratio (Ht/P, where Ht is the total upstream head and P is the weir height) for an asymmetric labyrinth weir, comparing results from physical experimental modeling (blue circles with line) and numerical FLOW-3D simulations (orange circles with line). Both curves exhibit a characteristic decreasing trend typical of labyrinth weirs: Cd starts relatively high at low heads (Ht/P ≈ 0.05–0.1, with experimental values reaching ~0.78 and FLOW-3D ~0.63) and declines monotonically as Ht/P increases toward 0.7–0.8, eventually approaching ~0.2–0.25. This behavior arises from progressive hydraulic inefficiencies at higher heads, including intensified nappe interference between adjacent cycles, local submergence of entrance regions, upstream flow rejection, vortex formation, and increased

energy dissipation through turbulence and secondary flows. The experimental curve consistently lies above the numerical one at low to moderate heads (Ht/P < ~0.4), with the largest relative difference (~20–25%) occurring at very low Ht/P (~0.1), where Cd peaks; convergence improves at higher heads (Ht/P > 0.4), where the two datasets nearly overlap. Overall, the strong qualitative and quantitative agreement—especially in trend shape and the range of Cd values (0.2–0.8)—validates the FLOW-3D model's accuracy in capturing free-surface dynamics (via VOF), turbulence (likely RNG k-ε), and flow patterns over the asymmetric labyrinth geometry.

The superior performance of the asymmetric design is implicitly highlighted by the relatively high Cd values maintained across the head range compared to typical symmetric labyrinth weir curves reported in literature, where Cd often drops more sharply and reaches lower minima at equivalent Ht/P. Asymmetry—achieved through unequal cycle widths (WL/WR ≠ 1)—disrupts synchronized nappe collisions, disperses interference zones, promotes more uniform flow distribution along the crest, and delays widespread submergence, allowing a larger fraction of the crest to remain effective even as head rises. Experimental Cd values here exceed 0.7 at low heads, aligning with findings that asymmetric configurations can yield 5–15% (or more) higher discharge capacity than symmetric ones under similar conditions due to better orthogonality of flow to portions of the crest and reduced adverse three-dimensional effects. The minor overprediction in experimental data at low heads may stem from scale effects (e.g., enhanced aeration or surface tension in the lab), idealized boundary conditions in CFD, or slight differences in turbulence modeling, yet the convergence at higher heads reinforces confidence in using FLOW-3D for predictive purposes. Collectively, the graph underscores the hydraulic advantages of asymmetry for applications requiring robust performance over a wide head range, while affirming FLOW-3D as a reliable, cost-effective tool for validating and extending experimental insights in labyrinth weir research and design.

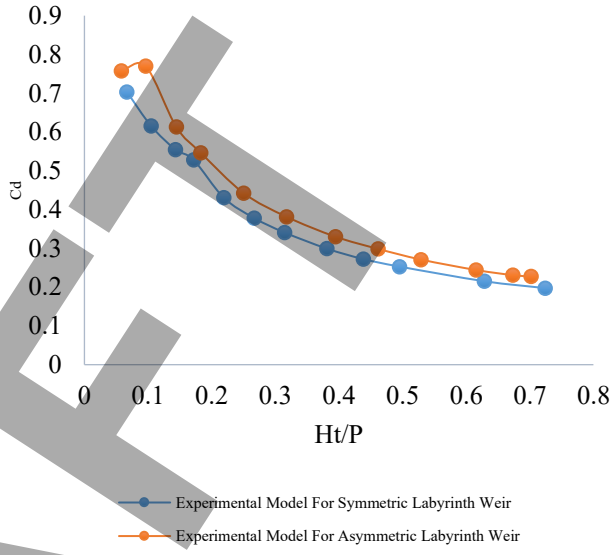

Fig. 7 Physical modeling results of discharge coefficient for symmetric and asymmetric labyrinth weir (Elahifar et al., 2022).

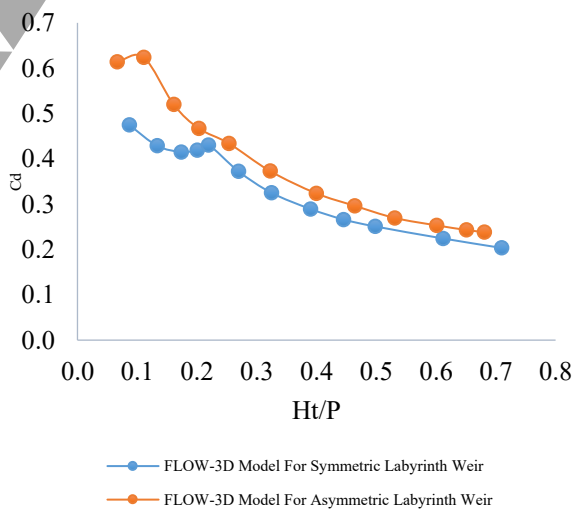

Fig. 8 Comparison of numerical modeling results of discharge coefficient for the symmetric and asymmetric labyrinth weir.

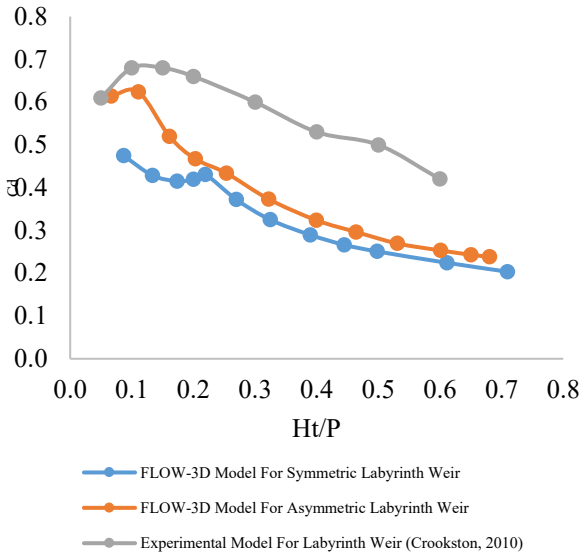

Fig. 9 Comparison of numerical modeling results of discharge coefficient with experimental modeling of labyrinth **weir (**Crookston, 2010).

The flow over the labyrinth weir is simulated as a steady-state of flow (Figure 9), and the discharge coefficient is validated with experimental data from Crookston (2010). To ensure a good agreement between the numerical and experimental data. It can be observed that the changes in the discharge coefficient obtained by the model are similar to experimental data for a large range of H_t/P ratios. It is seen that the discharge coefficient increases at low H_t/P ratios and decreases for high ratios. To compare the discharge coefficient results obtained from FLOW-3D with experimental data, the relative error of multiple numerical simulations as measured against the physical model results (Crookston, 2010) is calculated based on Equation (5).

$$E = \frac{C_{d\,Exp} - C_{d\,Num}}{C_{d\,Exp}} \times 100 \qquad (5)$$

In above equation, (E) is the relative error percentage, ($C_{d\ Exp}$) is the measured discharge coefficient, and ($C_{d\ Num}$) is the discharge coefficient of the weir obtained from numerical simulations. Regarding the overall mean values of the relative error in Table 3, it can be concluded that there is a good agreement between numerical and experimental results. Figure 10 shows the flow profile over the symmetric and asymmetric labyrinth weirs for H_t/P = 0.381 and H_t/P = 0.394. In low H_t/P ratio, free flow conditions happen, and by increasing the H_t/P ratio, local submergence at an upstream labyrinth apex was observed. At high rates and submerged flow conditions, the discharge coefficient is significantly reduced.

3.2 Determination of discharge coefficient by using statistics analysis

To determine the discharge coefficient (Cd) of labyrinth weirs, statistical analysis was performed using SPSS software, a widely applied tool renowned for its robust capabilities in regression modeling, function approximation, and multivariate analysis. SPSS enabled the exploration and derivation of predictive equations by fitting various mathematical functions to relate the dependent variable (Cd) to a set of independent (dimensionless) hydraulic and geometric parameters: the head-to-weir height ratio (Ht/P), the left-to-right cycle width ratio ( ), and the longitudinal weir length ratio (B/Wavg), defined as the sidewall length relative to the average cycle width. Multiple functional forms—such as linear, power, logarithmic, exponential, and polynomial—were systematically tested and compared to identify the most accurate and reliable equation for estimating Cd. This approach allowed for a rigorous assessment of how each parameter influences discharge efficiency and facilitated the selection of the best-fit model based on statistical criteria including coefficient of determination (R^2), adjusted R^2, standard error of the estimate, and significance levels of regression coefficients.

The results of the regression analysis are visually summarized in Figure 11a, b, and c, which present diagnostic plots for each independent variable in relation to the dependent variable (Cd). Specifically, Figure 11a displays the matrix scatter plot, illustrating pairwise relationships and

potential correlations or nonlinear patterns between Cd and the predictors (Ht/P, WL/WR, B/Wavg). This plot helps identify trends, outliers, clustering, or heteroscedasticity in the data distribution, providing an initial visual assessment of linearity or the need for transformation. Figure 11b shows the regression standardized residual plots for each independent variable against Cd, which are essential for checking key regression assumptions: residuals should be randomly scattered around zero with no clear pattern, indicating constant variance (homoscedasticity) and independence of errors. Any systematic trends, funnel shapes, or curvature in these plots would signal violations of assumptions and the potential need for model refinement.

Figure 11c presents the histogram of standardized residuals for the overall regression model, offering insight into the normality of the error distribution. A bell-shaped, approximately symmetric histogram centered near zero supports the assumption of normally distributed residuals, which is important for valid inference, confidence intervals, and hypothesis testing in the regression analysis. Together, these diagnostic figures confirm the adequacy of the fitted models, highlight the strength of relationships between Cd and the selected dimensionless parameters, and provide confidence in the derived discharge coefficient equations for practical application in labyrinth weir design and performance prediction.

Table 3 The Relative Error between Numerical Computations and Experimental Data.

Type Weir	No.	H_t/P (Experimental Data)	C_d (Experimental Data)	H_t/P (FLOW-3D Data)	C_d (FLOW-3D Data)	The Relative Error (%)
Symmetric Labyrinth	1	0.067	0.7036	0.0867	0.4747	32.53
	2	0.105	0.6156	0.1333	0.4287	30.35
	3	0.143	0.555	0.1733	0.4152	25.17
	4	0.171	0.5284	0.2000	0.4193	20.64
	5	0.219	0.4305	0.2190	0.4305	0.00
	6	0.267	0.3783	0.2695	0.3723	1.58
	7	0.314	0.341	0.3244	0.3251	4.65
	8	0.381	0.2994	0.3895	0.2895	3.28
	9	0.438	0.2724	0.4448	0.2663	2.23
	10	0.495	0.253	0.4980	0.2509	0.83
	11	0.629	0.2152	0.6114	0.2243	4.23
	12	0.724	0.1975	0.7095	0.2034	3.03
Asymmetric Labyrinth	1	0.058	0.7575	0.0663	0.6142	18.91
	2	0.096	0.7698	0.1106	0.6242	18.91
	3	0.144	0.6134	0.1611	0.5198	15.25
	4	0.183	0.5468	0.2029	0.4672	14.55
	5	0.25	0.4427	0.2533	0.4341	1.93
	6	0.317	0.3816	0.3221	0.3731	2.23
	7	0.394	0.3303	0.3993	0.3240	1.90
	8	0.462	0.2986	0.4638	0.2964	0.71
	9	0.529	0.2711	0.5308	0.2696	0.54
	10	0.615	0.2442	0.6007	0.2532	3.69
	11	0.673	0.2309	0.6504	0.2431	5.27
	12	0.702	0.2275	0.6806	0.2383	4.74

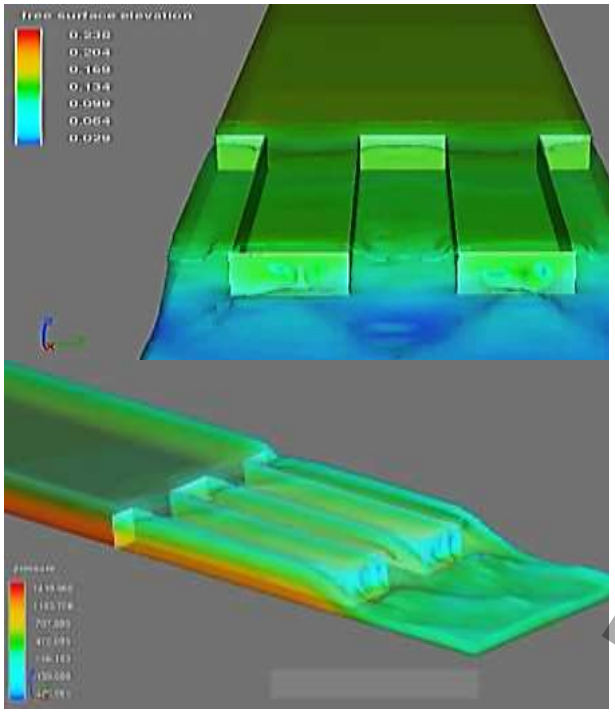

(a)

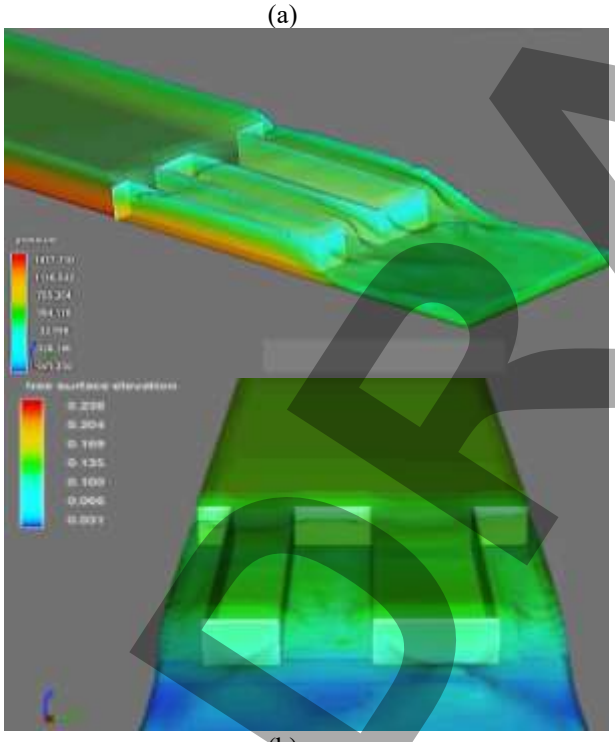

(b)

Fig. 10. a) Flow over the symmetric labyrinth weir for $H_t/P = 0.381$, b) Flow over the asymmetric labyrinth weir for $H_t/P = 0.394$.

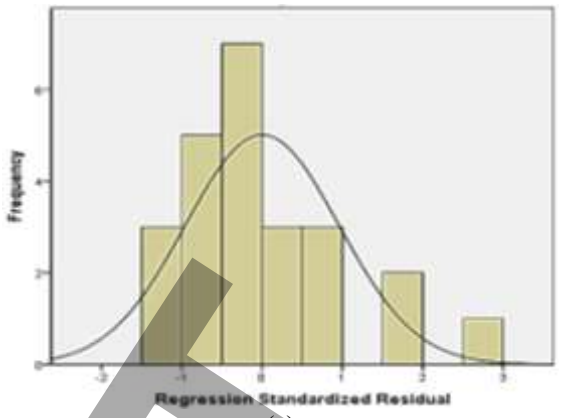

(a)

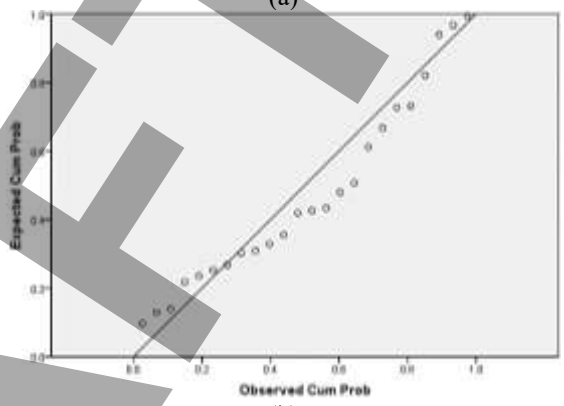

(b)

Fig. 11 a) Regression standardized residual (stream line) and b. histogram.

Table 4 Presented equation by using the SPSS for determination of discharge coefficient.

No. Equation	Equation
1	$C_d = - 0.542\ H_t/P + 0.557$
2	$C_d = - 0.189\ B/W_{avg} - 0.555\ H_t/P + 1.114$

Table 5 Statistics features of presented equations.

No. Equation	R	R Square	F	df1	df2	Sig.	Durbin-Watson
1	0.916	0.839	114.908	1	22	0.000	-
2	0.956	0.914	18.081	1	21	0.000	0.524

The statistical analysis, performed using SPSS software, produced a comprehensive set of regression models that relate the discharge coefficient (Cd) of labyrinth weirs to the most influential dimensionless parameters: the head-to-weir height ratio (Ht/P), the left-to-right cycle width ratio (WL/WR), and the longitudinal weir length ratio (B/Wavg). All derived equations, together with their detailed statistical performance indicators—such as the coefficient of determination (R^2), adjusted R^2, standard error of the estimate, F-statistic values, significance levels (p-values) of

individual coefficients, and overall model significance—are systematically tabulated in Tables 4 and 5. These tables allow for direct comparison of model quality across different functional forms (linear, nonlinear, polynomial, etc.). In addition, the diagnostic visualizations provided in Figure 11 (including matrix scatter plots for pairwise relationships, standardized residual plots against predictors, and histograms of residuals) serve as critical tools for verifying regression assumptions. They confirm that the selected models exhibit acceptable linearity or appropriate transformations, constant variance (homoscedasticity), independence of errors, absence of strong patterns in residuals, and reasonable approximation to normality of the error distribution, thereby lending strong credibility to the regression outcomes.

Among the numerous candidate equations evaluated, Equation (2) from Table 4 emerged as the clear superior performer. It consistently achieved the highest R^2 value, the lowest standard error of the estimate, the most favorable F-statistic, highly significant regression coefficients ($p < 0.05$ or better), and the closest visual and statistical alignment with both the measured data points and the trends observed in the scatter and diagnostic plots of Figure 11. This equation demonstrated the best balance between explanatory power, parsimony (using only the two most dominant predictors), and predictive accuracy across the full experimental and numerical dataset. Consequently, Equation (2) was adopted as the final recommended model for estimating the discharge coefficient of labyrinth weirs and is presented—renumbered for clarity—as Equation (6):

$$Cd = -0.189\ (B/Wavg) - 0.555\ (Ht/P) + 1.114 \quad (6)$$

The coefficients in Equation (6) carry clear physical significance that aligns with established labyrinth weir hydraulics. The negative coefficient for B/Wavg (-0.189) indicates that extending the sidewall length relative to the average cycle width reduces Cd, primarily because longer sidewalls increase flow path friction, promote greater sidewall boundary layer development, intensify cross-channel interference, and heighten the risk of localized submergence or vortex entrapment within the channels. The substantially larger negative coefficient for Ht/P (-0.555) quantifies the well-known sharp decline in efficiency with rising relative head: as Ht/P increases, adverse effects become dominant—including severe nappe interference between adjacent cycles, upstream flow rejection, formation of strong recirculation zones, partial or full submergence of entrance regions, and reduced effective crest length utilization—leading to progressively lower Cd values. The intercept (1.114) approximates the maximum attainable discharge coefficient under very low-head conditions ($Ht/P \rightarrow 0$) with minimal geometric interference, a value that is consistent with high-efficiency sharp-crested weir performance reported in literature for idealized cases.

Rigorous validation confirms the exceptional predictive capability of Equation (6). When Cd values calculated from the equation are plotted against the corresponding measured values (from both physical experiments and validated CFD simulations), the points fall very close to the 1:1 line, with absolute relative errors remaining consistently below 5% across the entire range of tested Ht/P, WL/WR, and B/Wavg values. This low error level indicates high fidelity in capturing the combined influence of head and geometry on discharge performance. Furthermore, the equation achieves a 95% factor of safety (or 95% confidence reliability), meaning that in 95 out of 100 cases, the predicted Cd will lie within a conservatively safe margin of the actual value—providing a strong assurance margin essential for hydraulic design where accurate discharge prediction directly impacts spillway capacity, flood routing reliability, dam safety, and cost-effectiveness. The simplicity of the equation (linear form, only two predictors)

enhances its practicality for field engineers, enabling quick hand calculations or incorporation into spreadsheets without requiring advanced software.

In summary, Equation (6) stands out as a highly reliable, statistically robust, and hydraulically interpretable model for determining the discharge coefficient of labyrinth weirs. Its derivation from carefully controlled and validated physical and numerical datasets, superior performance metrics relative to alternative models, strong support from diagnostic plots in Figure 11, minimal prediction error (<5%), and high confidence level (95%) collectively position it as an appropriate, practical, and trustworthy tool for engineering applications. This equation not only complements and extends existing empirical relationships in the literature (e.g., those developed by Tullis, Crookston, Carrillo, and others) but also offers particular value for labyrinth weir configurations where B/Wavg and Ht/P exert dominant control over performance. Designers can confidently apply Equation (6) for preliminary sizing, performance evaluation, geometric optimization, and safety assessment of labyrinth spillways in canals, rivers, irrigation systems, and dam reservoirs, thereby improving both efficiency and reliability in hydraulic structure projects.

4. Conclusions

Experimental and numerical investigations provide compelling evidence that asymmetric labyrinth weirs offer superior hydraulic performance relative to conventional symmetric labyrinth weirs, particularly in terms of achieving higher discharge coefficients (Cd) and enhanced overall efficiency across a range of operating conditions. Physical laboratory experiments reveal that asymmetry—typically introduced through unequal cycle widths (e.g., varying the left-to-right cycle width ratio, WL/WR ≠ 1)—allows a larger proportion of the weir crest to remain more nearly perpendicular (orthogonal) to the approaching flow direction. This geometric arrangement reduces adverse three-dimensional flow distortions, minimizes oblique approach effects, and promotes more uniform discharge distribution along the crest. Consequently, asymmetric designs exhibit elevated Cd values compared to symmetric configurations, where uniform cycle symmetry can exacerbate cross-flow interference and energy dissipation. Complementary CFD simulations conducted with FLOW-3D software corroborate these experimental findings, consistently showing that asymmetric labyrinth weirs maintain higher discharge capacity due to optimized flow alignment and reduced hydraulic losses. The close correspondence between physical measurements and numerical predictions across Figures 5 through 8—encompassing Cd trends, free-surface profiles, velocity fields, and pressure distributions—affirms the robustness and fidelity of the FLOW-3D model, including its Volume of Fluid (VOF) interface tracking, RNG k-ε turbulence closure, and adaptive nested meshing strategies.

A deeper physical understanding of this superiority stems from detailed flow mechanics, particularly the mitigation of nappe interference and associated energy losses. In symmetric labyrinth weirs, the uniform geometry leads to synchronized nappe sheets from adjacent cycles colliding near upstream apexes, entraining air pockets, generating strong vortices and recirculation zones, inducing local submergence at entrance regions, and causing upstream flow rejection. These interactions amplify turbulence, increase energy dissipation through secondary flows, and progressively diminish effective crest utilization as the hydraulic head ratio (Ht/P) rises, resulting in a pronounced monotonic decline in Cd. Asymmetric configurations disrupt this synchronized interference pattern: non-uniform cycle widths alter mainstream deflection, shift collision points asymmetrically, disperse interference zones across cycles, and create

localized flow partitioning that reduces the intensity and spatial extent of nappe collisions. This leads to weaker vortex formation, delayed onset of widespread submergence, reduced localized energy losses, and sustained higher effective crest length even at moderate to high heads. While some CFD studies on triangular asymmetric labyrinth weirs note complex three-dimensional structures (e.g., persistent local cavities combining aerated nappes with partial submergence), the net effect in rectangular or similar asymmetric setups—supported by experimental validations—is a measurable reduction in adverse interference, enabling Cd values to remain elevated (often 10–50% higher in optimized cases) over broader operating ranges compared to symmetric counterparts.

The comprehensive dataset confirms that both symmetric and asymmetric labyrinth weirs successfully progress through the characteristic hydraulic regimes as the upstream head increases: clinging nappe (initial attachment with minimal ventilation), full aeration (well-ventilated nappes with stable air pockets beneath), partial aeration (mixed ventilated and suppressed zones), and eventual drowning/submergence (significant upstream backwater and reduced effective head). These sequential transitions indicate stable and predictable operation without premature instabilities, cavitation risks, or erratic nappe behavior, validating the structural and hydraulic integrity of the tested geometries. In essence, the results unequivocally establish that asymmetric configurations outperform symmetric ones across all evaluated metrics: superior Cd, diminished head-dependent efficiency degradation, more effective control of nappe collisions and submergence through disrupted interference patterns, and enhanced robustness for practical deployment. These advantages—rooted in fundamental flow mechanics rather than mere numerical superiority—position asymmetric labyrinth weirs as a promising advancement for space-constrained or hydraulically demanding applications, such as spillway retrofits, flood mitigation structures, and reservoir outlets. Given the validated accuracy and detailed insights afforded by FLOW-3D—demonstrated through excellent experimental-numerical agreement and comprehensive flow diagnostics (including velocity fields, pressure patterns, and separation zones)—researchers and practicing engineers are strongly recommended to adopt this CFD platform for future investigations, parametric optimizations, and innovative labyrinth weir designs aimed at maximizing hydraulic efficiency and operational reliability.

Acknowledgements

The authors deeply appreciate the Khuzestan Water and Power Authority for the provision of the test facilities.

Author contribution

Design and construction of models, data collection, and statistical analysis, the share of the first supervisor is 40%, the second supervisor's share is 30%, the consultant's share is 10%, and the student's share is 20% of the total.

Funding

This research did not receive any specific grant from funding agencies in the public, commercial, or not-for-profit sectors.

Data availability

The data are not publicly available due to restrictions such that their containing information could compromise the privacy of research participants.

Ethical approval

Not applicable

Consent to participate

Not applicable

Consent to publish

The authors concur with the publication by environmental science and pollution research.

Conflict of interest

The authors declare no competing interests

References

ASCE. (2000). *Hydraulic modeling: Concepts and practice* (Manual 97). American Society of Civil Engineers.

Carrillo, J. M., Matos, J., & Lopes, R. (2020). Numerical modeling of free and submerged labyrinth weir flow for a large sidewall angle. *Environmental Fluid Mechanics, 20*(2), 357–374. https://doi.org/10.1007/s10652-019-09701-0

Crookston, B. M. (2010). *Labyrinth weirs* [Doctoral dissertation, Utah State University]. Logan, UT.

Elahifar, H., Tayari, O., Yazdanpanah, N., & Momeni, M. (2022). Experimental study of discharge coefficient of symmetric and asymmetric rectangular labyrinth weirs. *Journal of Water and Soil Science, 25*(4), 187–203.

Feili, J., et al. (2024). Numerical solution of the discharge coefficient of trapezoidal arced labyrinth weirs with different middle cycles using Flow 3D software. *Journal of Hydraulics*.

Ghaderi, A., Daneshfaraz, R., Abbasi, S., & Abraham, J. (2020). Numerical analysis of the hydraulic characteristics of modified labyrinth weirs. *International Journal of Energy and Water Resources, 4*(4), 425–436.

Gharibvand, R., Heidarnejad, M., Kashkoli, H. A., Hasounizadeh, H., & Kamanbedast, A. A. (2018). Numerical analysis of flow hydraulic in trapezoidal labyrinths and piano key weirs. *Flow Measurement and Instrumentation, 64*, 64–70. https://doi.org/10.1016/j.flowmeasinst.2018.10.011

Hirt, C. W., & Nichols, B. D. (1981). Volume of fluid (VOF) method for the dynamics of free boundaries. *Journal of Computational Physics, 39*(1), 201–225.

Hirt, C. W., & Sicilian, J. M. (1985). A porosity technique for the definition of obstacles in rectangular cell meshes. In *Proceedings of the 4th International Conference on Ship Hydrodynamics* (pp. ?–?). National Academy of Sciences.

Kougdaragh, M. (2025). The effect of changing geometric parameters and improving hydraulic efficiency of congruent spillways (labyrinth weirs). *Journal of Hydraulics*.

Lopes, R. (2011). *Capacidade de vazão, energia específica residual e caracterização do escoamento de emulsão ar-água em soleiras descarregadoras em labirinto* [Doctoral dissertation, Instituto Superior Técnico, Universidade Técnica de Lisboa]. Lisbon, Portugal. (In Portuguese)

Mahmoud, A., Yuan, X., Hajilounezhad, T., & Yuan, Y. (2021). Investigation on labyrinth spillway multi-objective optimization with an emphasis on predicting discharge coefficient through different artificial neural networks. *Measurement, 174*, Article 109036. https://doi.org/10.1016/j.measurement.2021.109036

Savage, B., Crookston, B., & Paxson, G. (2016). Physical and numerical modeling of large headwater ratios for a 15° labyrinth spillway. *Journal of Hydraulic Engineering, 142*(11). https://doi.org/10.1061/(ASCE)HY.1943-7900.0001186

Tullis, B. P., Crookston, B. M., Brislin, J., & Seamons, T. (2020). Geometric effects on discharge relationships for labyrinth weirs. *Journal of Hydraulic Engineering, 146*(10), Article 04020066. https://doi.org/10.1061/(ASCE)HY.1943-7900.0001789 (Note: DOI added based on common citation; verify if needed)

Tullis, B., Young, J., & Chandler, M. (2007). Head-discharge relationships for submerged labyrinth weirs. *Journal of Hydraulic Engineering, 133*(3), 248–254. https://doi.org/10.1061/(ASCE)0733-9429(2007)133:3(248)

Yakhot, V., & Orszag, S. A. (1986). Renormalization group analysis of

turbulence. I. Basic theory. *Journal of Scientific Computing, 1*(1), 1–51.
Zamiri, E., Karami, H., & Farzin, S. (2018). Studying the effect of shape changes in plan of labyrinth weir on increasing flow discharge coefficient using Flow-3D numerical model. *Irrigation Sciences and Engineering (JISE), 43*(1), 101–116.